AECL-7789

ATOMIC ENERGY
OF CANADA LIMITED

L'ENERGIE ATOMIQUE
DU CANADA, LIMITEE

# A STUDY OF THE EFFECT OF CIRCUMFERENTIAL TEMPERATURE VARIATIONS ON FUEL-SHEATH STRAIN IN AN INERT ATMOSPHERE

# ETUDE DES EFFETS DES VARIATIONS DE TEMPERATURE CIRCONFERENTIELLES SUR LES CONTRAINTES DES GAINES DE COMBUSTIBLE DANS UNE ATMOSPHERE INERTE

J. Ferner, R. K. Rondeau, H. E. Rosinger

Whiteshell Nuclear Research Establishment

Etablissement de recherches nucléaires de Whiteshell

Pinawa, Manitoba R0E 1L0

July 1983 juillet

10

ATOMIC ENERGY OF CANADA LIMITED

# A STUDY OF THE EFFECT OF CIRCUMFERENTIAL TEMPERATURE VARIATIONS ON FUEL-SHEATH STRAIN IN AN INERT ATMOSPHERE

by

J. Ferner, R.K. Rondeau and H.E. Rosinger

Whiteshell Nuclear Research Establishment
Pinawa, Manitoba ROE 1L0
1983 July

AECL-7789

ÉTUDE DES EFFETS DES VARIATIONS DE TEMPÉRATURE CIRCONFÉRENTIELLES SUR LES CONTRAINTES DES GAINES DE COMBUSTIBLE DANS UNE ATMOSPHÈRE INERTE

par

J. Ferner, R.K. Rondeau et H.E. Rosinger

## RESUMÉ

On a mis au point un modèle de rupture des gaines de combustible en Zircaloy-4 qui a servi à prédire les effets des variations de température circonférentielles ($\Delta T$) sur le comportement des contraintes des gaines de combustible en atmosphère inerte. De plus, des données expérimentales ont été produites pour les ruptures de gaine de combustible dans les régions de phase $\alpha$- et $(\alpha+\beta)$-, qu'on a comparées aux prédictions du modèle.

Il en découle que, tant dans le cas des données expérimentales que des prédictions du modèle, l'accroissement de $\Delta T$ réduit la contrainte que subit la gaine. La diminuation de la contrainte de rupture que provoque une augmentation de $\Delta T$ a lieu principalement entre les premiers 15 K à 20 K. Dans le cas de valeurs $\Delta T$ élevées, les contraintes de rupture des régions de phase $\alpha$- et $(\alpha+\beta)$ tendent vers une valeur asymptotique de l'ordre de 5 à 20%, quelque soit le taux de chauffage et la variation de température circonférentielle.

L'Énergie Atomique du Canada, Limitée
Établissement de recherches nucléaires de Whiteshell
Pinawa, Manitoba ROE 1L0
1983 juillet

AECL-7789

# A STUDY OF THE EFFECT OF CIRCUMFERENTIAL TEMPERATURE VARIATIONS ON FUEL-SHEATH STRAIN IN AN INERT ATMOSPHERE

by

J. Ferner, R.K. Rondeau and H.E. Rosinger

## ABSTRACT

A failure model for Zircaloy-4 fuel sheaths has been developed and used to predict the effect of circumferential temperature variations ($\Delta T$) on fuel-sheath strain behaviour in an inert atmosphere. In addition, experimental data were generated for fuel-sheath failures in the $\alpha$- and $(\alpha+\beta)$-phase regions and compared to the predictions of the model.

For both the experimental data and the model predictions it was found that increasing $\Delta T$ decreases sheath strain. Most of the reduction in burst strain with increasing $\Delta T$ occurs in the first 15 K to 20 K. For high $\Delta T$ values, burst strains in the $\alpha$- and $(\alpha+\beta)$-phase regions tend to an asymptotic value in the range 5 to 20%, irrespective of both heating rate and circumferential temperature variation.

Atomic Energy of Canada Limited
Whiteshell Nuclear Research Establishment
Pinawa, Manitoba ROE 1LO
1983 July

AECL-7789

# CONTENTS

# 1. INTRODUCTION

In the analysis of hypothetical loss-of-coolant accidents (LOCAs) in CANDU reactors*, calculations have indicated that the Zircaloy-4 fuel sheaths will be subjected to a rise in temperature and a differential pressure as the primary cooling circuit depressurizes. Such conditions may cause plastic deformation and eventually failure of the fuel sheath. The fuel-sheath deformation (i.e. the total circumferential strain) will dictate the amount of coolant flow restriction in the fuel channel. The time at which the fuel sheath fails will determine the maximum deformation and will indicate the time when fission products will be released into the cooling system. Since the degree of coolant flow restriction and the timing of the fission-product release are important factors in determining the consequences of postulated accident scenarios, it is important to understand the mechanisms that affect sheath behaviour so that accurate predictions can be made.

One factor known to have a significant effect on fuel-sheath strain is the existence of a temperature variation around the circumference of the sheath. Previous studies, such as the German REBEKA[1-4] and U.S. MRBT[5-7] programs, have demonstrated the significance of circumferential temperature variation on sheath burst strain. The horizontal nature of the fuel channels in the CANDU reactor system will impose a circumferential temperature variation on the fuel sheath and thus a study of the effects of circumferential temperature variation has important implications for CANDU reactor safety.

This particular study of the effect of circumferential temperature variation ($\Delta T$) on sheath strain consisted of three main parts:

1. Experiments were performed to generate a set of burst strain ($\epsilon_{\theta B}$) versus $\Delta T$ data. These data were compared to another independent data set[8].

---

* CANada Deuterium Uranium

2. The failure model[9-14] for Zircaloy fuel sheathing, in the form of the BURST-2[15] computer program, was used in a parametric study to predict the effect of various parameters on sheath burst strain.

3. The experimental data generated were compared to the BURST-2 predictions.

The major purpose of this study was to provide a detailed understanding of the effect of ΔT on sheath burst strain and to further verify the fuel-sheath failure model and associated computer code.

## 2. COMPONENTS OF THE STUDY

### 2.1 EXPERIMENTAL

The experiments performed, though similar to hypothetical LOCA conditions, were idealized and considerably simplified. This simplified both the experimental procedure and the computer prediction of sheath behaviour. In particular, instead of the complicated pressure and temperature sequences that might accompany a postulated LOCA, the sheath was subjected to a uniform temperature ramp at a constant differential pressure in an inert atmosphere.

#### 2.1.1 Equipment

The main apparatus is shown schematically in Figure 1. The fuel element simulator consists of an internal heater, hollow alumina pellets and the fuel sheath. The alumina pellets had the same outside diameter (∼ 14.3 mm) as the $UO_2$ pellets in a CANDU fuel element; the central hole was 6.1 mm diameter, to accommodate the heater snugly without binding. The fuel sheaths were regular Zircaloy-4 sheathing with outside diameters of 15.21 mm to 15.24 mm, a wall thickness of approximately 0.43 mm and a length of

491 mm. The internal heater heated the central 300 to 350 mm of the sheath length. The inside of the sheath was pressurized with helium while the glass enclosure was evacuated.

Three experimental configurations were used to produce varying degrees of circumferential temperature variation. These were:

1. The partial heating shroud, shown in Figure 1, was used to produce high $\Delta T$ values by applying external heating to one side of the sheath. Temperature variations of 150 K and more were produced in this way.

2. Without shroud heating, medium and small $\Delta T$ values (typically 10 K to 50 K) were produced, possibly due to asymmetric heat flow from the heater to the sheath.

3. To minimize the circumferential temperature variation, a completely encircling shroud was placed around the sheath. With this shroud, $\Delta T$ values of 10 K and less were obtained.

Sheath temperatures were monitored by small chromel-alumel thermocouples spot welded onto the sheath exterior. Two main thermocouple configurations, shown in Figure 2, were adopted for these experiments. The eight-thermocouple arrangement was used for low-temperature tests and gave a reasonable indication of the temperature distribution on the sheath. However, for higher temperature tests, the four-thermocouple configuration was used to prevent excessive heat conduction from the sheath via the thermocouple wires. To prevent eutectic formation between the thermocouples and the sheath at temperatures above about 1240 K, pads of 0.025-mm thick niobium foil were placed between the sheath and the thermocouples.

The power to the internal heater was controlled by a programmable controller which regulated the temperature at thermocouple #1 (see Figure 2). All data generated during a test were recorded on a PDP-11 data logger for subsequent analysis.

### 2.1.2 Procedure

The tests were designed to produce sheath failure in each of the three phases of Zircaloy-4. From the failure model, it is known that the temperature at which a fuel sheath fails can be controlled by the initial stress on the fuel sheath. Therefore, by using a graph such as Figure 3, generated from BURST-2, or by using BURST-2 directly, the internal pressures required for the various experiments were pre-calculated:

1. An internal pressure near 3.5 MPa (initial stress of approximately 64 MPa) was used to cause failure near 1023 K (750°C), in the α-phase region.

2. A pressure near 1.2 MPa (initial stress of 20 MPa) was used to cause failure near 1183 K (910°C), in the (α+β)-phase region.

3. A pressure of approximately 0.23 MPa (initial stress of about 4 MPa) was used to cause failure near 1323 K (1050°C), in the β-phase region. Since tests in this phase region are still under way, the data are not presented in this report.

Before each test, the sheath was measured in length, outside diameter, and wall thickness. Ten-centimetre gauge marks were made along the length of the sheath, near its centre. Also, the thermocouple placement positions were marked on the sheath. The apparatus was assembled, the vessel evacuated, and the test begun.

Once all power was on and the internal pressure set to the desired value, the programmable controller maintained a temperature ramp of 1 $K \cdot s^{-1}$ while the pressure remained reasonably constant. Temperatures and the pressure inside the sheath were recorded at half-second intervals from approximately 300 s to 500 s preceding sheath failure to about 100 s to 200 s after failure.

The final experimental results were obtained as follows. First, the burst (failure) time, as shown by a sudden pressure drop, was obtained from the computer plot of internal sheath pressure. Knowing the burst time, the approximate burst temperature was obtained from the temperature plot. Then $\Delta T$ was determined from a simultaneous plot of all thermocouple temperatures. The temperature variation at a particular axial position on the sheath was found from the separation between the temperature curves of diametrically opposite thermocouples. $\Delta T$ was then taken as the average of the values at the different axial positions. The error bars for $\Delta T$ were determined by considering the spatial variations in temperature that existed in the burst region. Finally, the burst strain was determined by comparing the final expanded circumference of the sheath in the burst region with the initial unstrained circumference.

### 2.1.3 Experimental Results

The experimental values of burst strain versus circumferential temperature variation for the $\alpha$-phase tests are presented in Figure 4. Also shown are data from an independent study[8]. Several general trends are evident. First, the figure shows that very small circumferential temperature variations resulted in very large burst strains and very large $\Delta T$ values yielded much smaller burst strains. The data also show that the major decrease in burst strain occurs over the first 15 K to 20 K, whereas decreases in burst strain for further increases in $\Delta T$ are considerably less. For example, for $\Delta T$ values of less than 10 K, burst strains of more than 130% were obtained, whereas for $\Delta T$ values of greater than 20 K, burst strains did not exceed 50%, and were generally in the 20% to 40% range. Burst strains then remained approximately constant for $\Delta T$ up to 150 k and more, showing almost asymptotic behaviour at higher $\Delta T$ values.

As indicated in Section 2.1.1, the very small $\Delta T$ values, and hence the large burst strains, were produced only when the encircling shroud was around the sheath. Burst strains were considerably less without this shroud.

The macrographs in Figure 5 show typical failures produced in the α-phase region for two different values of ΔT. For nearly uniform circumferential temperature, i.e. small ΔT, the sheath deformed by uniform ballooning and finally failed via a pinhole. For very high ΔT, however, sheath deformation was restricted to a small section facing the heating shroud, with failure occurring as a rapid and often violent burst of the deformed section, usually resulting in a large hole. The macrographs clearly show these failure characteristics.

The experimental data for the (α+β)-phase tests are presented in Figure 6. These data show the same trend of decreasing burst strain with increasing ΔT, with the majority of the decrease occurring in the first 20 K. For very high ΔT values (>50 K), the burst strain tends to an asymptotic value near 15% to 25%.

Macrographs of typical failures in the (α+β)-phase for both low and high circumferential temperature variations are shown in Figure 7. For a low ΔT, the sheath showed a small amount of uniform ballooning, but still failed with a burst on the hotter side of the sheath. When a high ΔT was imposed on the sheath, only slight overall deformation was noted. Failure of the sheath in this case again consisted of a burst on the hot side.

Comparison of the results from both phase regions allows further observations to be made. First, the α-phase tests generally exhibit higher burst strains than do the (α+β)-phase tests. This is most clearly evident when comparing the results for low ΔT values: the α-tests produced strains >130%, whereas the (α+β)-tests did not exceed 60% total strain. This difference is not as significant at higher ΔT values. Furthermore, the types of failures illustrated by the macrographs indicate that the (α+β)-phase is much more sensitive to a hot spot than is the α-phase. This is shown by the localized burst and minimal ballooning exhibited by the failure in the (α+β)-phase.

## 2.2 PARAMETRIC STUDY

The sheath-failure model has usually been applied to a fuel sheath subjected to a uniform circumferential temperature distribution. However, when the temperature around the circumference of the sheath is not uniform, the basic equations of the failure model will not apply to the sheath as a whole. In such a case, the temperature distribution must be approximated by a number of finite angular elements, each with a unique but uniform temperature. The failure model can then be applied to each element individually, with sheath failure occurring when the failure criterion is met by one of the angular elements. The application of the failure model to a sheath with an imposed $\Delta T$ would, therefore, be an excellent verification, since the model must be applied numerous times to the same sheath.

The BURST-2 computer code uses the multiple-angular-element method and can calculate sheath burst strain for arbitrary pressure and temperature sequences and any given circumferential temperature distribution on the sheath. In this study, BURST-2 was used to study the effect of certain parameters on sheath burst strain. The three main parameters considered were: the form of the temperature distribution, the rate at which the sheath is heated, and the anisotropy of Zircaloy-4 in the $\alpha$-phase region.

As for the experiments, the calculations were divided into three sections, each corresponding to failure in one of the three phase regions of Zircaloy-4. The failure temperatures used were the same as those quoted in Section 2.1.2, namely 1023 K (750°C), 1183 K (910°C), and 1323 K (1050°C). All computer simulations assumed an initial temperature of either 570 K or 590 K. The difference in these initial temperatures is unimportant as the creep behaviour of Zircaloy-4 at temperatures below 850 K is insignificant.

### 2.2.1 Effect of the Form of the Temperature Distribution

As mentioned in Section 2.1.1, problems with excessive heat conduction from the sheath via the thermocouples prevented a complete measurment of the circumferential temperature distribution at a particular axial position. Therefore, it was necessary to fit the experimental data to an assumed analytical function. The general form of the distribution chosen was:

$$T\ (\theta,t) = T(t) - \Delta T \left\{ \frac{1 + \cos\ (\theta + \pi)}{2} \right\}^{c} \qquad (1)$$

where
- T is temperature
- t is time
- ΔT is the maximum circumferential temperature variation
- θ is the angle around the sheath
- c is a constant

Using this equation, the shape of the temperature distribution around the sheath can be changed by adjusting c. A value of c=1.0 gives a sinusoidal distribution, a value of c=0.5 gives a more localized hotspot and c=2.0 gives a less localized hotspot. A graph of these three temperature distributions is given in Figure 8 for an arbitrary value of ΔT.

The calculated effect on burst strain of varying the temperature distribution is shown in Figures 4 and 6 for the α- and (α+β)-phase regions, respectively. The predicted effect for the β-phase region is shown in Figure 9. All three graphs show the same general trend in that all three temperature distributions show similar strain behaviour at low ΔT, but are significantly different at high ΔT values. In general, a more localized hotspot produces a more localized strain region, and even though the area of the sheath in the vicinity of the hotspot may have a very large strain, the greatly reduced strain on the remainder of the sheath causes the overall total strain to be reduced.

For the remainder of the parametric study, where the temperature distribution was not a parameter, a distribution corresponding to c=1.0 was chosen as the standard. This particular distribution was chosen because it gives reasonable agreement with the experimental data, as shown in Figures 4 and 6.

### 2.2.2 Effect of Heating Rate

A fuel sheath subjected to a uniform circumferential temperature shows significantly different strain behaviour for different heating rates. In particular, as heating rate increases, the total burst strain decreases. Heating rate is, therefore, an important parameter.

To assess the effect of heating rate on the burst strain in the presence of a circumferential temperature variation, four heating rates were assumed in the BURST-2 calculations: 1, 5, 10, and 50 $K \cdot s^{-1}$. The predicted results are shown in Figures 10 to 12. In agreement with previous results, the different heating rates result in different burst strains for uniform or small circumferential temperature variations. However, as $\Delta T$ increases, the predicted curves for the various heating rates tend to a similar asymptotic burst strain value. For the $\alpha$- and $(\alpha+\beta)$-phase regions, the asymptotic value is in the 5% to 20% range. For the $\beta$-phase region, the asymptotic value is in the 20% to 40% range. Thus, a large circumferential temperature variation tends to cancel the effect of heating rate.

### 2.2.3 Effect of Anistropy

The anisotropy of Zircaloy-4 fuel sheathing should be accounted for to predict properly the deformation in various directions. In previous BURST-2 studies, it had been assumed that the Zircaloy-4 sheathing was isotropic (F=G=H=0.5) in both the $(\alpha+\beta)$-and $\beta$-phase regions, whereas the $\alpha$-phase was assumed to be highly anisotropic (F=0.934, G=0.374, H=0.192). However, a separate study[16] has shown that the sheathing is nearly isotropic (F=0.56, G=0.48, H=0.46) in the $\alpha$-phase. Therefore, in a comparison of the two cases, both anisotropies were considered for a temperature ramp of 1 $K \cdot s^{-1}$, while assuming a sinusoidal (c=1.0) temperature distribution. The curves generated by BURST-2 are shown in Figure 13 for the $\alpha$-phase region. The nearly isotropic case results in slightly larger strains than the anisotropic case. For the $(\alpha+\beta)$-phase, the difference between the two curves is so small that they are essentially indistinguishable; the similarity is explained by the fact that the sheath does most of its straining in the few seconds just before failure. Thus, for failure in the (α+β)-region, both cases will do the majority of their straining in the region where they are isotropic and hence both will have similar strain behaviour.

# 3. DISCUSSION

## 3.1 COMPARISON OF THEORY WITH EXPERIMENT

The assumption of a sinusoidal temperature distribution ($c=1.0$) gave the best correlation with the experimental data for both the α-phase (Figure 4) and (α+β)-phase (Figure 6) regions. In the absence of a more refined method of measuring the sheath temperature (i.e. without thermocouples that conduct heat away from the sheath), direct and accurate verification of the sinusoidal temperature distribution will be basically impossible and this theoretical/experimental correlation must serve as satisfactory verification.

Several of the failed fuel sheaths were metallographically examined and the change in wall thickness around the circumference measured at the axial burst location. Figure 14 is a comparison between BURST-2 predictions and the wall thickness strain as a function of angular position on the sheath circumference, for two sheaths having different $\Delta T$ values. Due to bilateral symmetry, data for only half of the sheath are shown. In addition to the reasonable agreement between prediction and experiment, the figure shows the influence of circumferential temperature variation. For the sheath having the higher circumferential temperature variation, most of the strain occurs over a small portion of the circumference. The remainder of the sheath undergoes almost no strain. For the sheath having the lower circumferential temperature variation, most of the strain again occurs over a small portion of the circumference. However, the remainder of the sheath also undergoes some strain. The larger the circumferential temperature variation, the more localized the strain. Even though the localized strain in both cases may be large, the very small strain in the remainder of the sheath causes the total circumferential strain to be small.

The effect of heating rate (discussed in Section 2.2.2) could not be compared with experiment due to the lack of experimental data at heating rates greater than 1 $K \cdot s^{-1}$.

The effect of anisotropy (discussed in Section 2.2.3) is also well predicted particularly for failure in the α-phase region (shown in Figure 13). For the highly anisotropic case (F=0.934, G=0.374, H=0.192) the model tends to underpredict burst strains slightly, whereas for the nearly isotropic case (F=0.56, G=0.48, H=0.46) there is excellent agreement with the experimental data. This is further verification of the failure model and of the measured anisotropy coefficients.

## 3.2 POSSIBLE SOURCES OF ERROR

Although the correlation between theory and experiment is generally good, minor discrepancies exist. These, however, can probably be attributed to one or more of the following causes.

First, the burst strain of a sheath seems to be highly sensitive to the shape of the circumferential temperature distribution. Since this distribution is extremely difficult to measure, and since BURST-2 calculations rely on the shape of the distribution, accurate prediction of burst strain is made difficult. It is also possible that the actual distribution may vary slightly from test to test, due to assymmetries in the test apparatus, causing a general scattering of the experimental data.

In the BURST-2 calculations, and in comparison with experimental data, it was assumed that the temperature varied uniformly around the tube and that there were no sudden variations. Figure 15 shows the measured wall thickness strain around the sheath circumference for a specimen deformed in the α-phase region and having a measured circumferential temperature variation of 0±5 K. Even this specimen, which had an almost uniform temperature around the circumference, shows considerable variation in wall thickness strain, indicating localized temperature variations around the sheath circumference. Any such localized temperature variations would cause discrepancies between predictions and measurements.

Uncertainties in the measurement of $\Delta T$ and burst strain could also affect the data; most of this uncertainty is included in the error bars for the data.

The BURST-2 computer program also contains several potential sources of error. Many of the constants used in various equations in the program have been determined experimentally, and as a result, have some inherent error. Therefore, since BURST-2 calculations use different constants for different phase regions, it is possible that predictions by BURST-2 for one phase region may be quite accurate, but not be so accurate for a different phase region.

## 4. CONCLUSIONS

This study of the effect of circumferential temperature variations on fuel-sheath strain has presented some experimental results and a parametric computer study. The experiments subjected the fuel sheath to simple heating and pressure conditions, while the parametric study used the fuel-sheath failure model, in the form of the BURST-2 computer program, to predict fuel-sheath strain behaviour under these simplified conditions.

Within the limits of the study, the following conclusions may be drawn:

1. Increasing circumferential temperature variations result in decreasing sheath burst strains.

2. Most of the reduction in burst strain with increasing $\Delta T$ occurs in the first 15 K to 20 K. The reduction in strain for higher temperature variations is considerably less.

3. A circumferential temperature variation of less than 20 K is difficult to produce experimentally without enclosing the sheath in a shroud. Since this uniform heat flux situation is not likely to occur in a reactor, a reactor fuel sheath subjected to a similar heating cycle will probably always exhibit a circumferential temperature variation.

4. The shape of the temperature distribution on the fuel sheath is a very significant factor affecting burst strain, and more consistent prediction of burst strain may require a more detailed measurement of the circumferential temperature distribution. At present, conventional thermocouple measurements provide only limited information.

5. Both a high circumferential temperature variation and a highly localized hotspot on a sheath produce a localized region of strain in the vicinity of the burst. Even though the localized strain may be large, the very small strain in the remainder of the sheath causes the total circumferential strain to be small.

6. Low $\Delta T$ values and well-dispersed temperature distributions produce more uniform strains around the sheath circumference and, hence, a large overall strain.

7. Burst strains are larger for the $\alpha$-phase region than for the $(\alpha+\beta)$-phase region.

8. In an inert atmosphere, burst strains are predicted to be larger for the $\beta$-phase region than for the $\alpha$-phase region.

9. Varying the heating rate does not significantly affect the burst strain of a sheath subjected to a high $\Delta T$.

10. At high $\Delta T$ values, burst strains in the $\alpha$- and $(\alpha+\beta)$-phase regions tend to an asymptotic value in the range 5% to 20% (engineering

strain), i.e. provided $\Delta T$ is high enough, say 150 K, burst strains will be in the range of 5% to 20%, irrespective of both heating rate and $\Delta T$.

11. The anisotropy of Zircaloy-4 fuel sheathing in the $\alpha$-phase region has a minimal effect on sheath burst strain for failure in the $(\alpha+\beta)$- and $\beta$-phase regions.

## REFERENCES


1. F. Erbacher, H.J. Neitzel and K. Wiehr, "Interaction Between Thermohydraulics and Fuel Clad Ballooning in a LOCA, Results of REBEKA Multirod Burst Tests with Flooding", presented at the 6th Water Reactor Safety Research Information Meeting, Gaithersburg, Maryland, 1978.

2. F. Erbacher, H.J. Neitzel, M. Reimann and K. Wiehr, "Out-of-Pile Experiments on Ballooning in Zircaloy Fuel Rod Claddings in the Low Pressure Phase of a Loss-of-Coolant Accident", Specialists' Meeting on the Behaviour of Water Reactor Fuel Elements Under Accident Conditions, Spatind, Norway, 1976.

3. F. Erbacher, H.J. Neitzel, M. Reimann and K. Wiehr, "Ballooning in Zircaloy Fuel Rod Claddings in a Loss-of-Coolant Accident", Proceedings of the Topical Meeting on Thermal Reactor Safety, Sun Valley, Idaho, CONF-770708, 1977 July 31-August 4.

4. K. Wiehr, F.J. Erbacher and H.J. Neitzel, "Influence of Thermohydraulics on Fuel Rod Behaviour in a LOCA", CSNI Specislists' Meeting on Safety Aspects of Fuel Behaviour in Off-Normal and Accident Conditions, Espoo, Finland, 1980.

5. R.H. Chapman, "Preliminary Multirod Burst Test Program Results and Implications of Interest to Reactor Safety Evaluations", presented at the 6th Water Reactor Safety Research Information Meeting, Gaithersburg, Maryland, CONF-781146-4, 1978.

6. R.H. Chapman, J.L. Crowley, A.W. Longest and G. Hofmann, "Zircaloy Cladding Deformation in a Steam Environment with Transient Heating", American Society for Testing and Materials, ASTM STP 681, 391 (1979).

7. R.H. Chapman, "Results and Status of ORNL Single Rod and Multirod Bundle Tests in a Steam Environment", presented at the Joint US-NRC/-KfK-PNS LWR Safety Research Information Exchange Meeting, Karlsruhe, 1978.

8. P.E. Hynes, personal communication, 1982.

9. H.J. Neitzel and H.E.Rosinger, "The Development of a Burst Criterion for Zircaloy Fuel Cladding Under LOCA Conditions", Atomic Energy of Canada Limited Report, AECL-6420 (1980).

10. H.E. Rosinger, H.J. Neitzel and F.J. Erbacher, "The Development of a Burst Criterion for Zircaloy Fuel Cladding Under LOCA Conditions", Res. Mechanica 2, (1981).

11. R.L. Varty and H.E. Rosinger, "A Failure-criterion Model for Thin-walled Zircaloy-4 Tubes in the 900 to 1600K Temperature Range", in Fracture Problems and Solutions in the Energy Industry, L.A. Simpson, Ed., Pergamon Press, Oxford and New York, 1982, 135-143.

12. R.L. Varty and H.E. Rosinger, "Comparison of a Fuel Sheath Failure Model with Published Experimental Data", Atomic Energy of Canada Limited Report, AECL-6806 (1982).

13. F. Erbacher, H.J. Neitzel, H. Rosinger, H. Schmidt and K. Wiehr, "Burst Criterion of Zircaloy Fuel Claddings in a Loss-of-Coolant Accident", ASTM Fifth International Conference on Zirconium in the Nuclear Industry, American Society for Testing and Materials, ASTM STP 754, 271 (1982).

14. T. Cheung and H.E. Rosinger, "A Failure Criterion for Zircaloy Fuel Sheaths Under LOCA Conditions", Trans. of the 6th Inter. Conf. on Structural Mechanics in Reactor Technology, paper #3/6 (1981).

15. R.L. Varty, "User's Guide to BURST-1, A Program to Calculate the Failure of Fuel Sheaths During A Postulated LOCA", unpublished Whiteshell Nuclear Research Establishment Report, WNRE-504 (1981).

16. H.E. Rosinger, J. Bowden, R.S.W. Shewfelt, "The Anisotropic Creep Behaviour Zircaloy-4 Fuel Cladding at 1073 K", Atomic Energy of Canada Limited Report, AECL-6447 (1982).

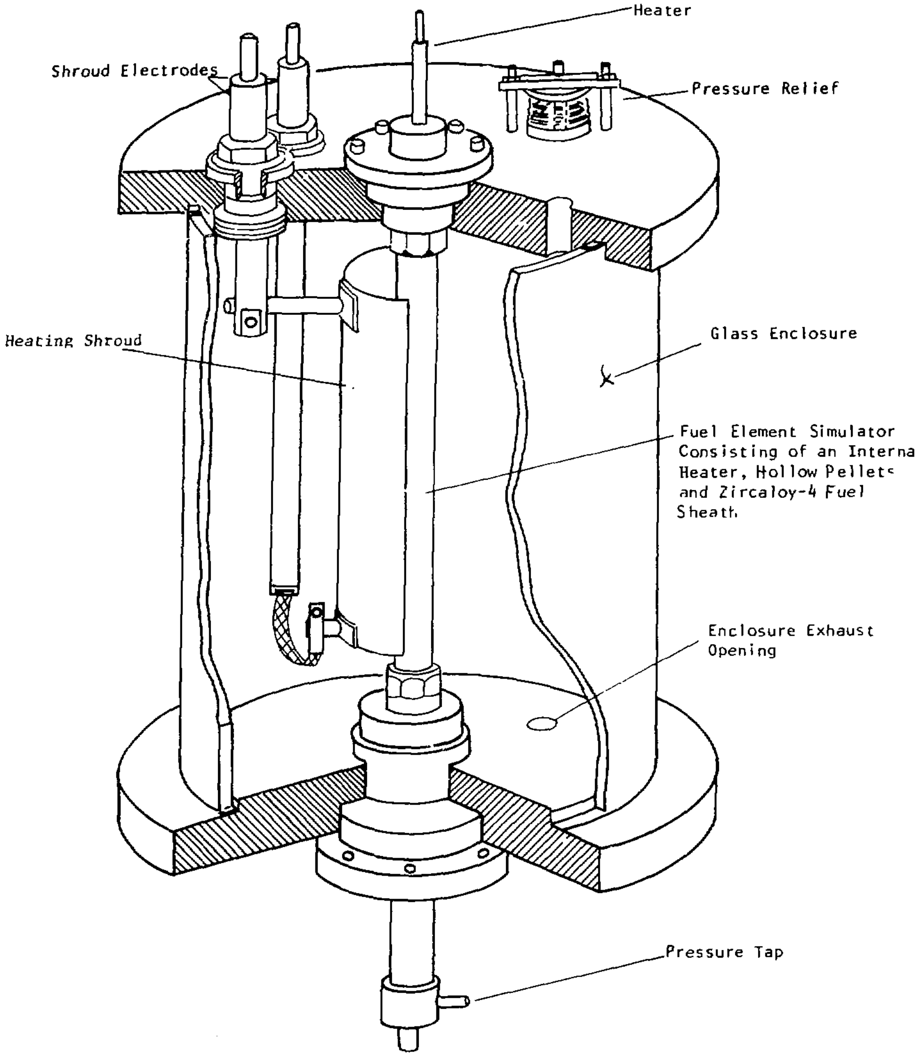


FIGURE 1: Schematic of the Experimental Vessel Used to Generate Circumferential Temperature Variations in Zircaloy-4 Fuel Sheathing

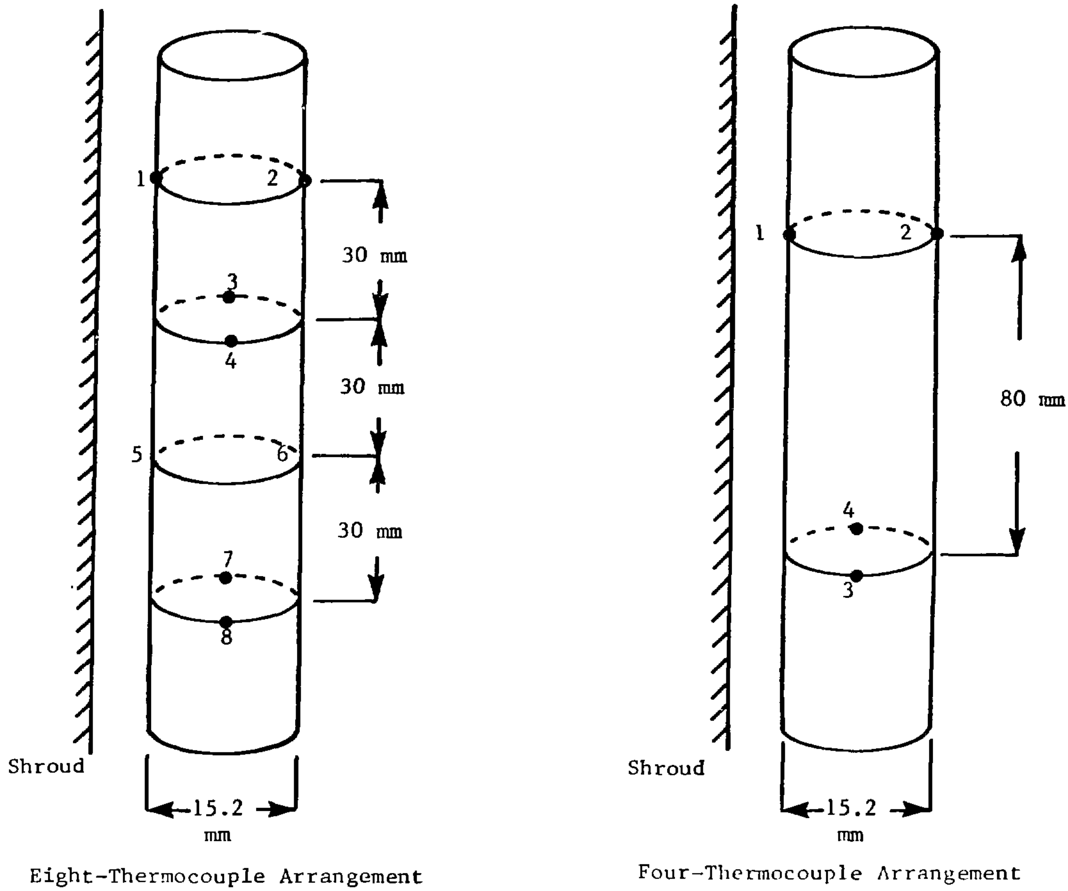


FIGURE 2: Schematic of the Thermocouple Arrangements Used in the Circumferential Temperature Variation Experiments

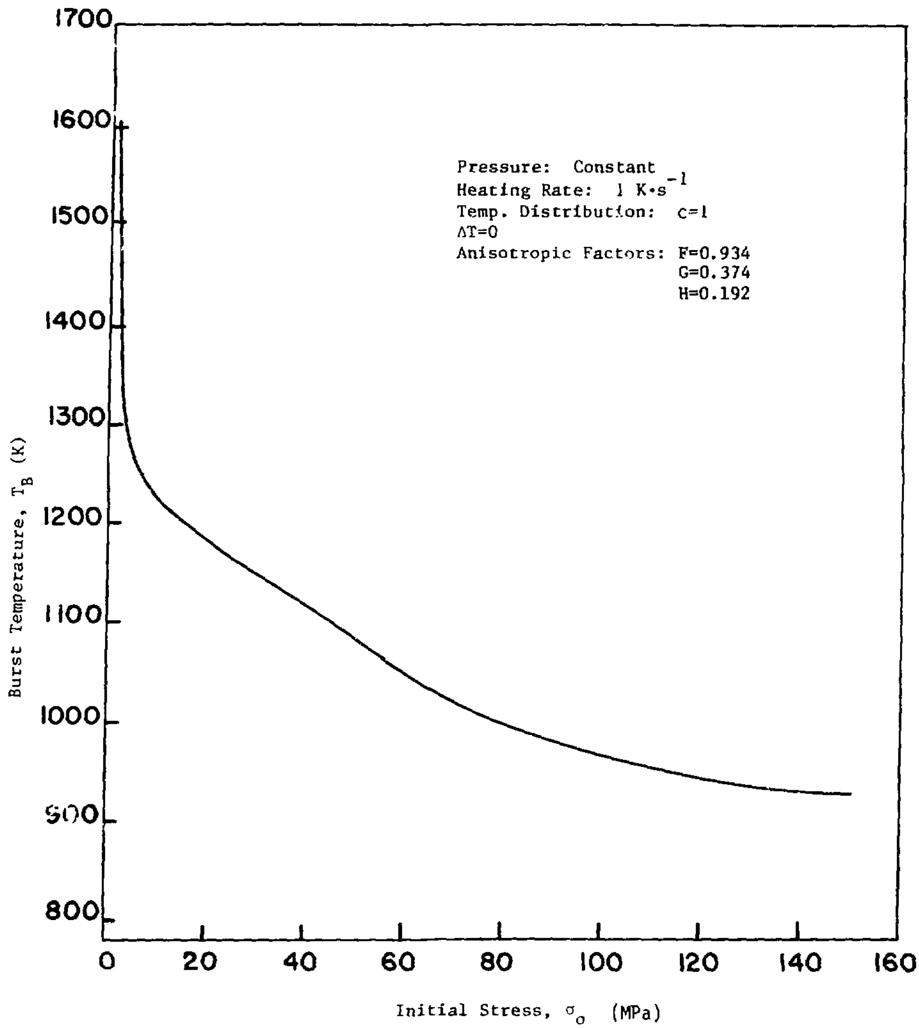


FIGURE 3: Predicted Burst Temperature Versus Initial Stress for a Heating Rate of 1 $K \cdot s^{-1}$

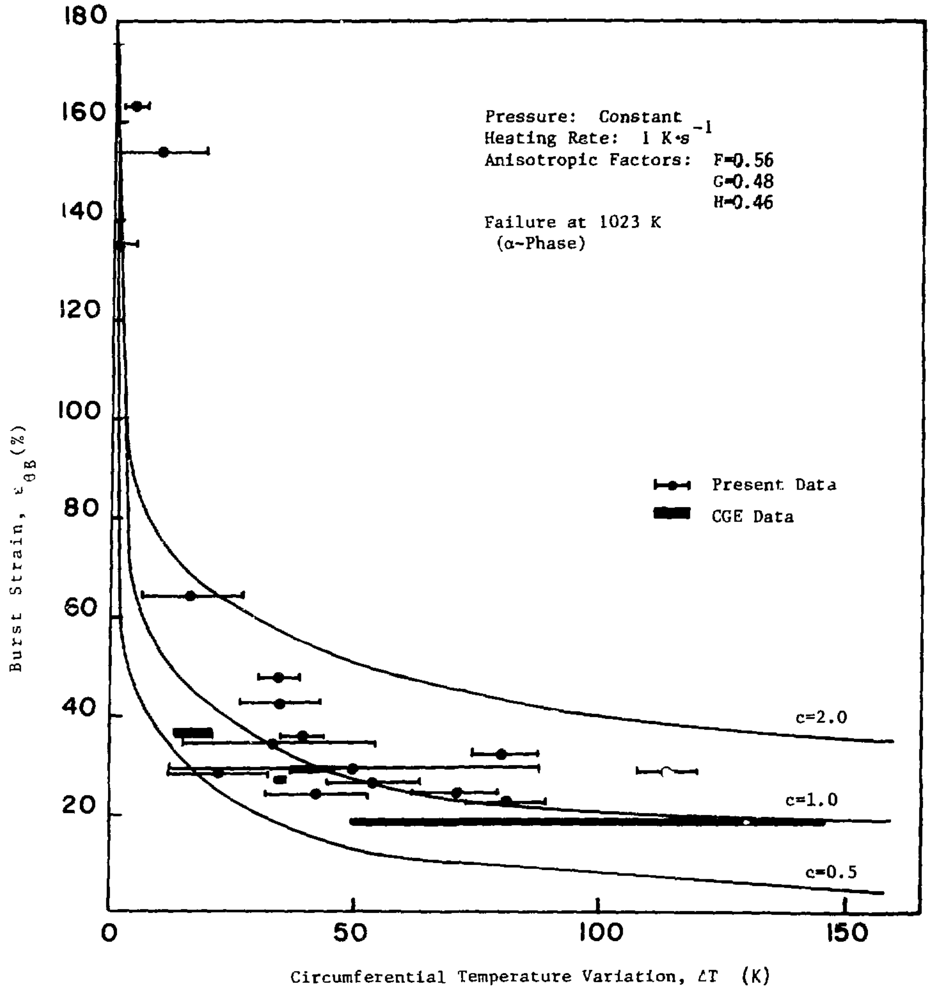


FIGURE 4: Experimental Burst Strain as a Function of the Circumferential Temperature Variation for Failure in the α-Phase Region (1023 K)

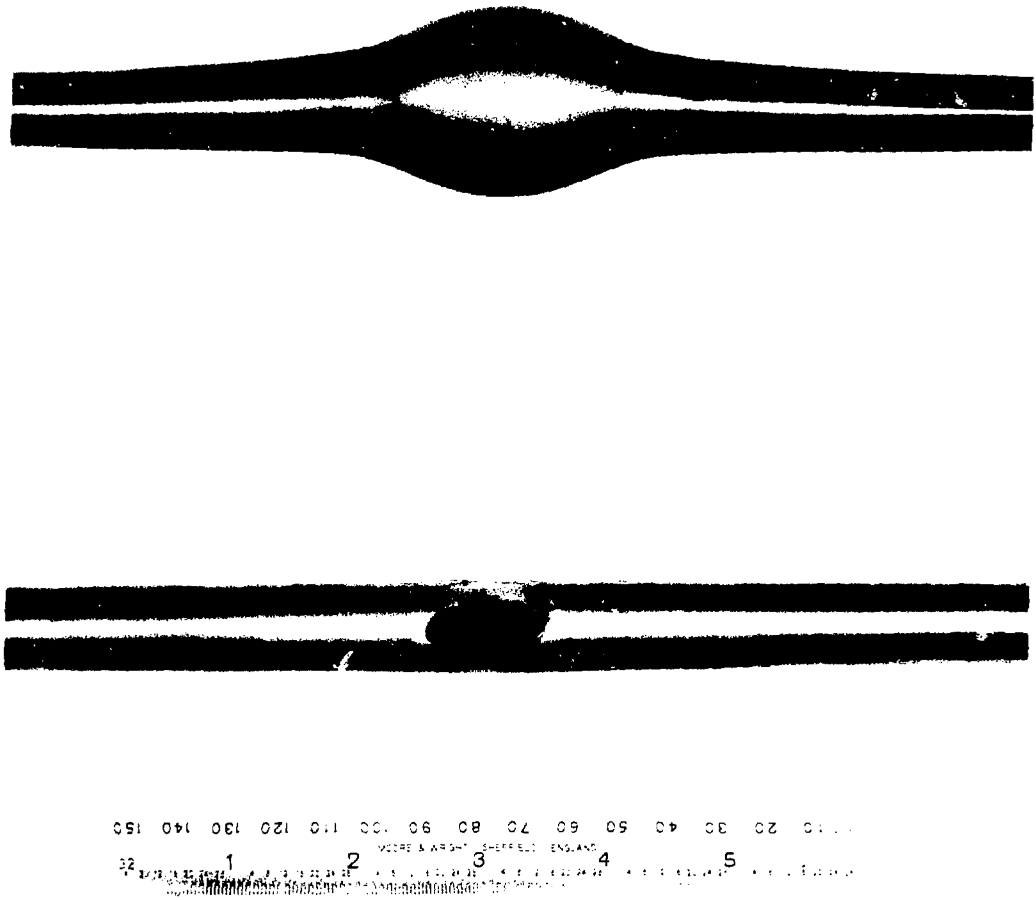

FIGURE 5: Typical Deformation and Failure Observed for α-phase Region Tests, with Small (top) and Large (bottom) Circumferential Temperature Variations

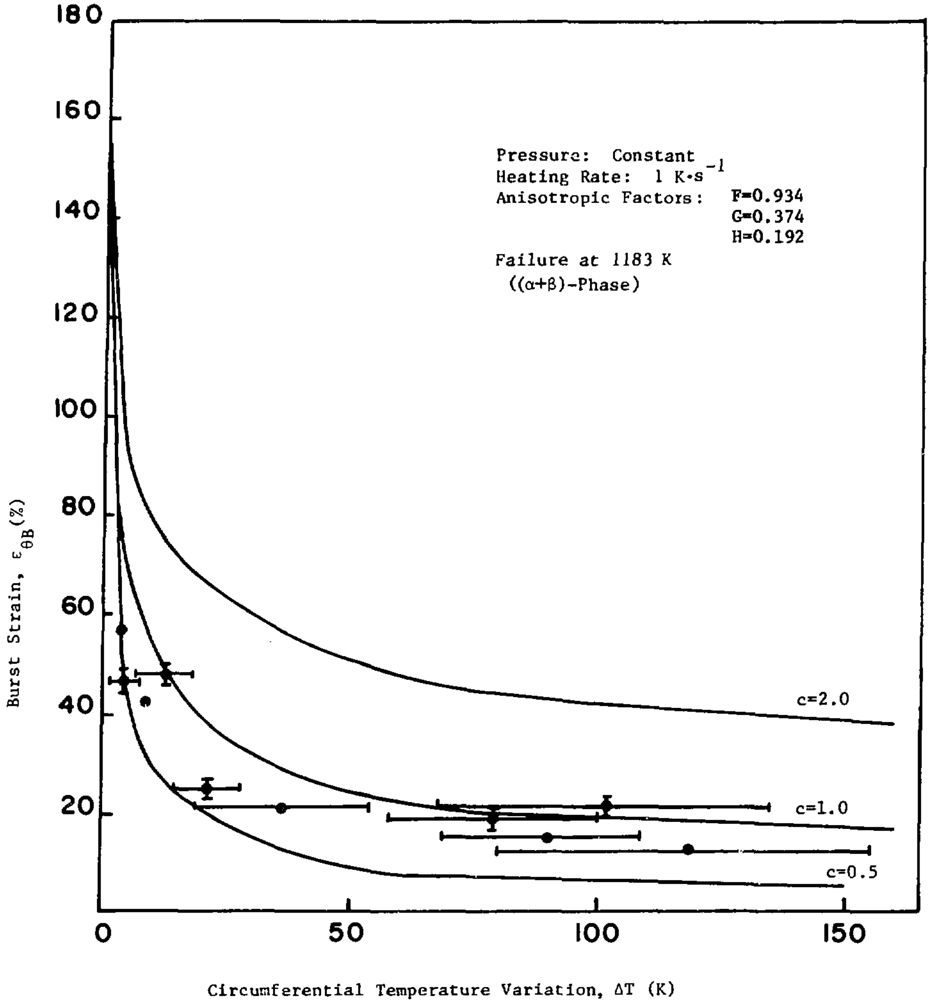


FIGURE 6: Experimental Burst Strain as a Function of the Circumferential Temperature Variation for Failure in the (α+β)-Phase Region (1183 K)

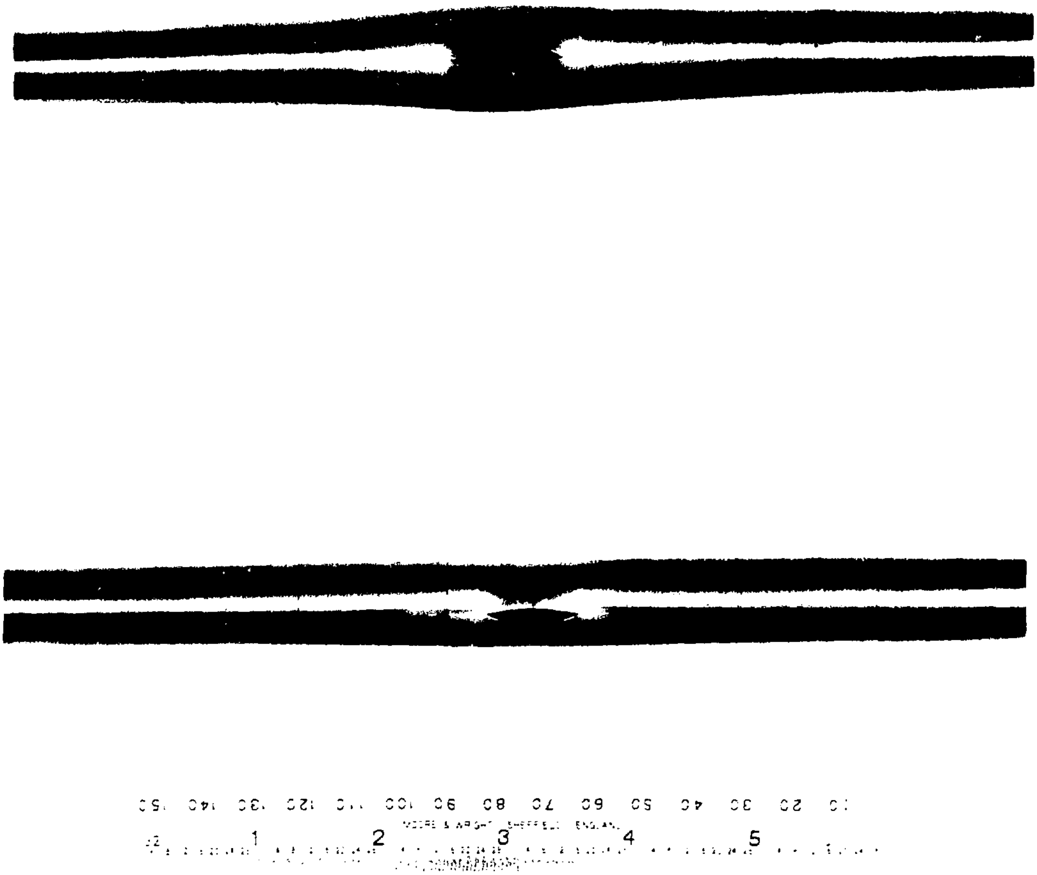

FIGURE 7: Typical Failures Observed in the $(\alpha+\beta)$-Phase Region with Small (top) and Large (bottom) Circumferential Temperature Variations

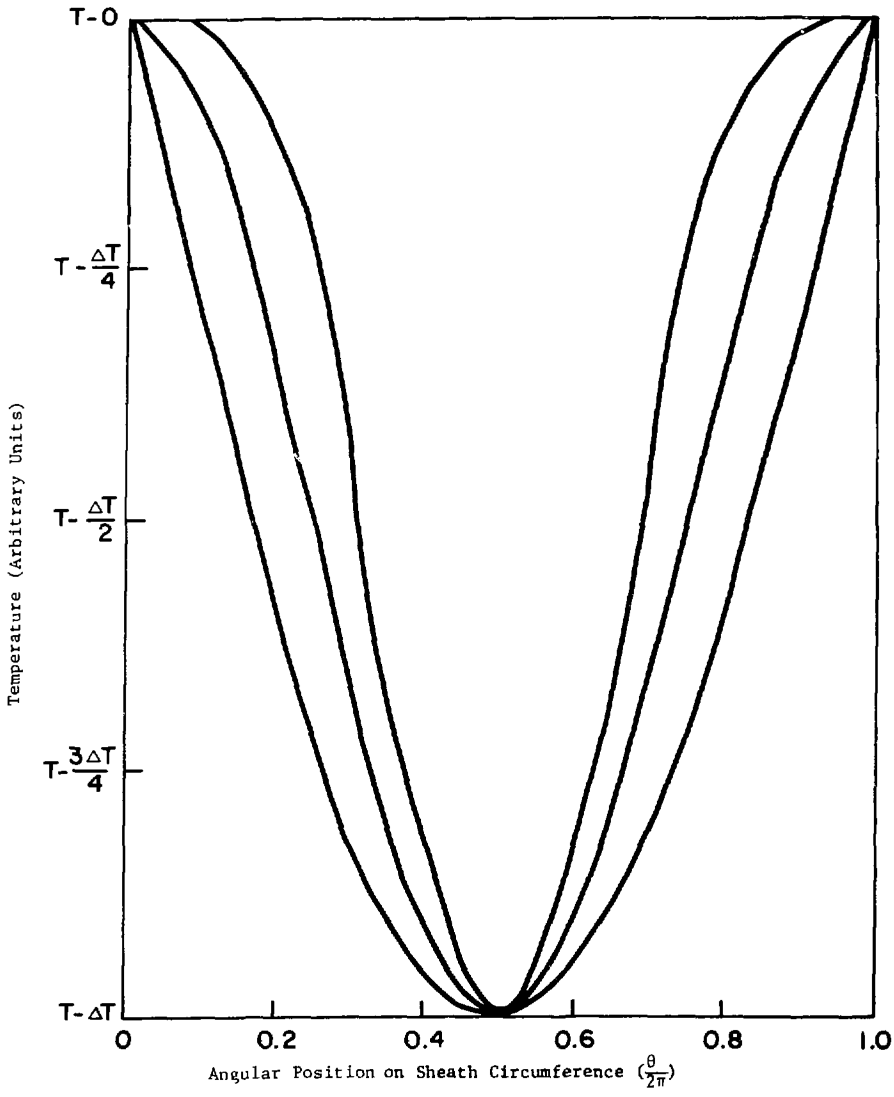


FIGURE 8: Temperature Distributions Around a Sheath for Arbitrary Values of Circumferential Temperature Variation

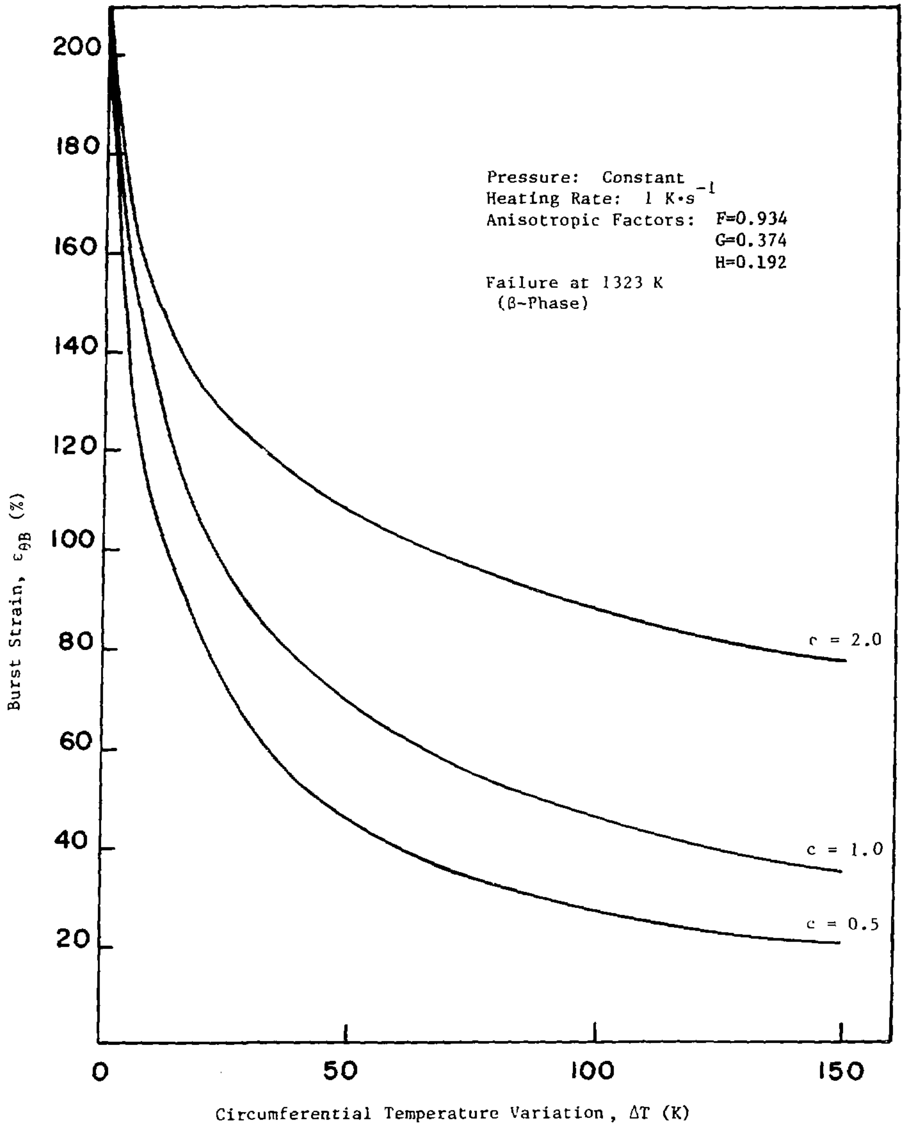


FIGURE 9: Predicted Burst Strain Versus Circumferential Temperature Variation for Failure in the β-Phase Region (1323 K)

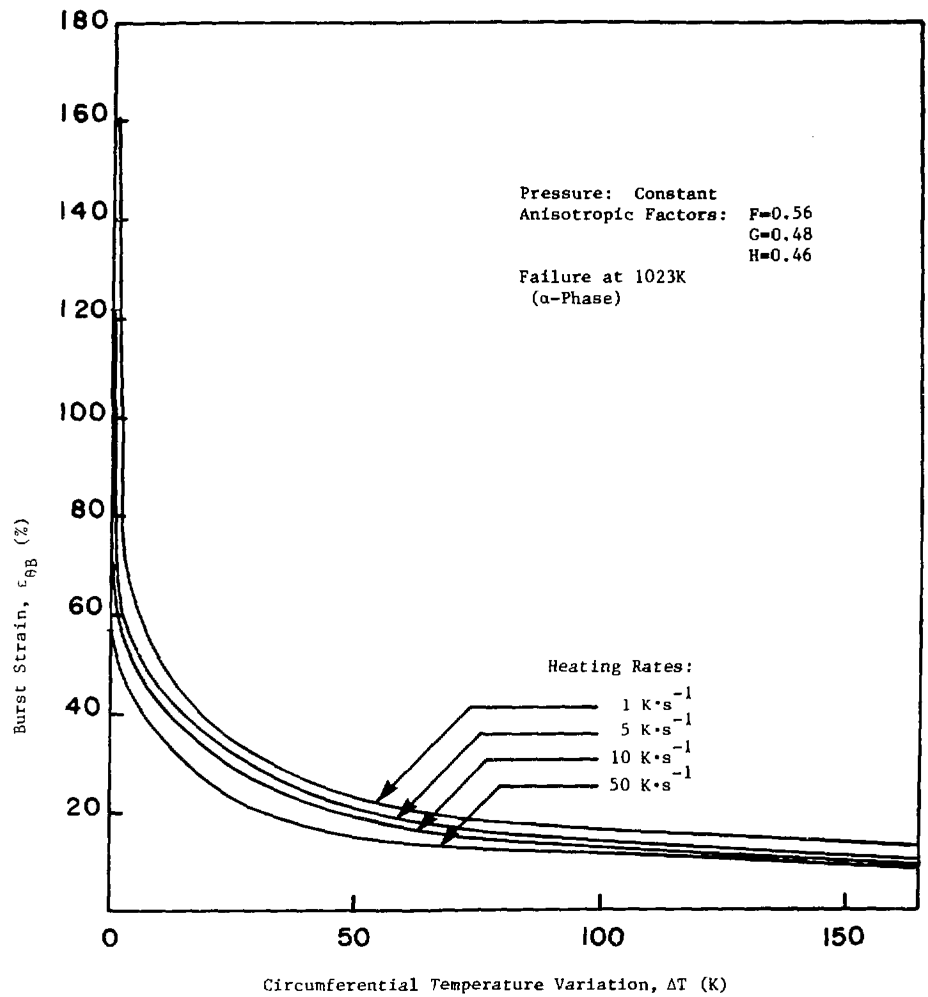


FIGURE 10: Effect of Heating Rate on the Burst Strain Versus Circumferential Temperature Variation for Failure in the α-Phase Region (1023 K)

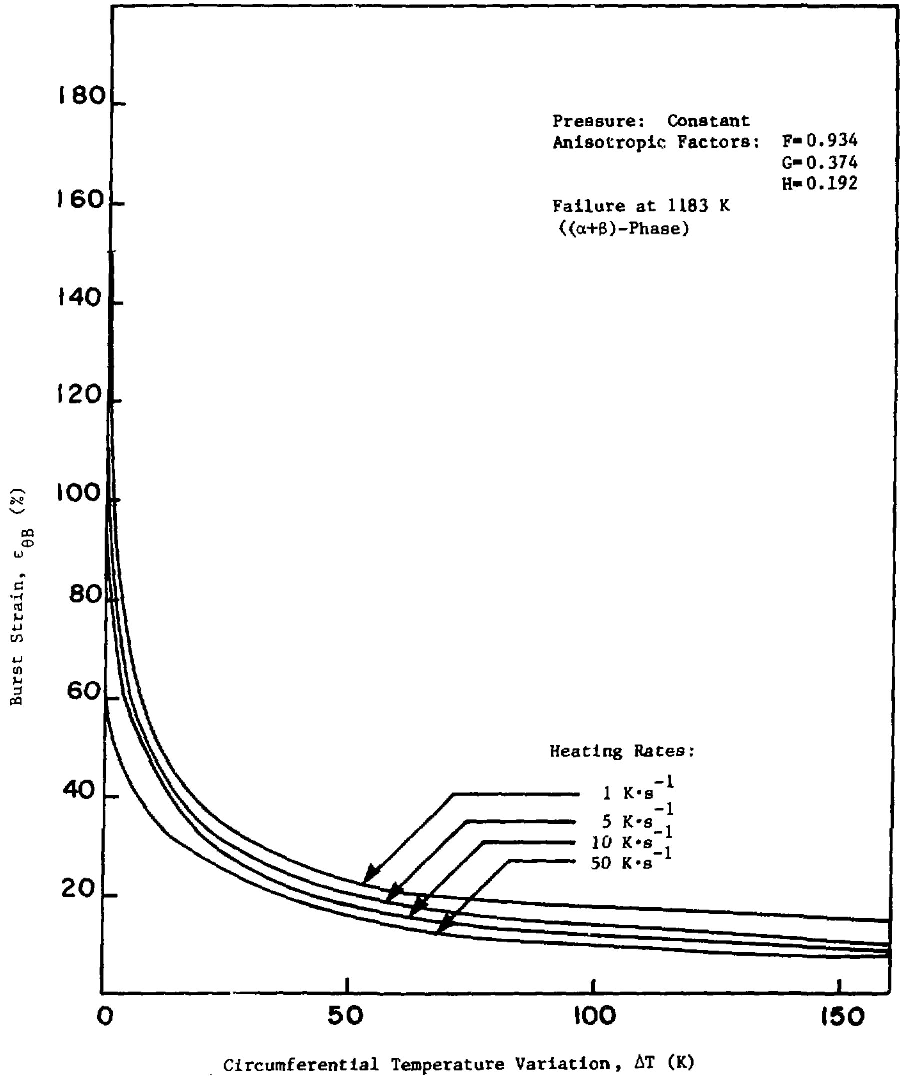


FIGURE 11: Effect of Heating Rate on the Burst Strain Versus Circumferential Temperature Variation for Failure in the (α+β)-Phase Region (1183 K)

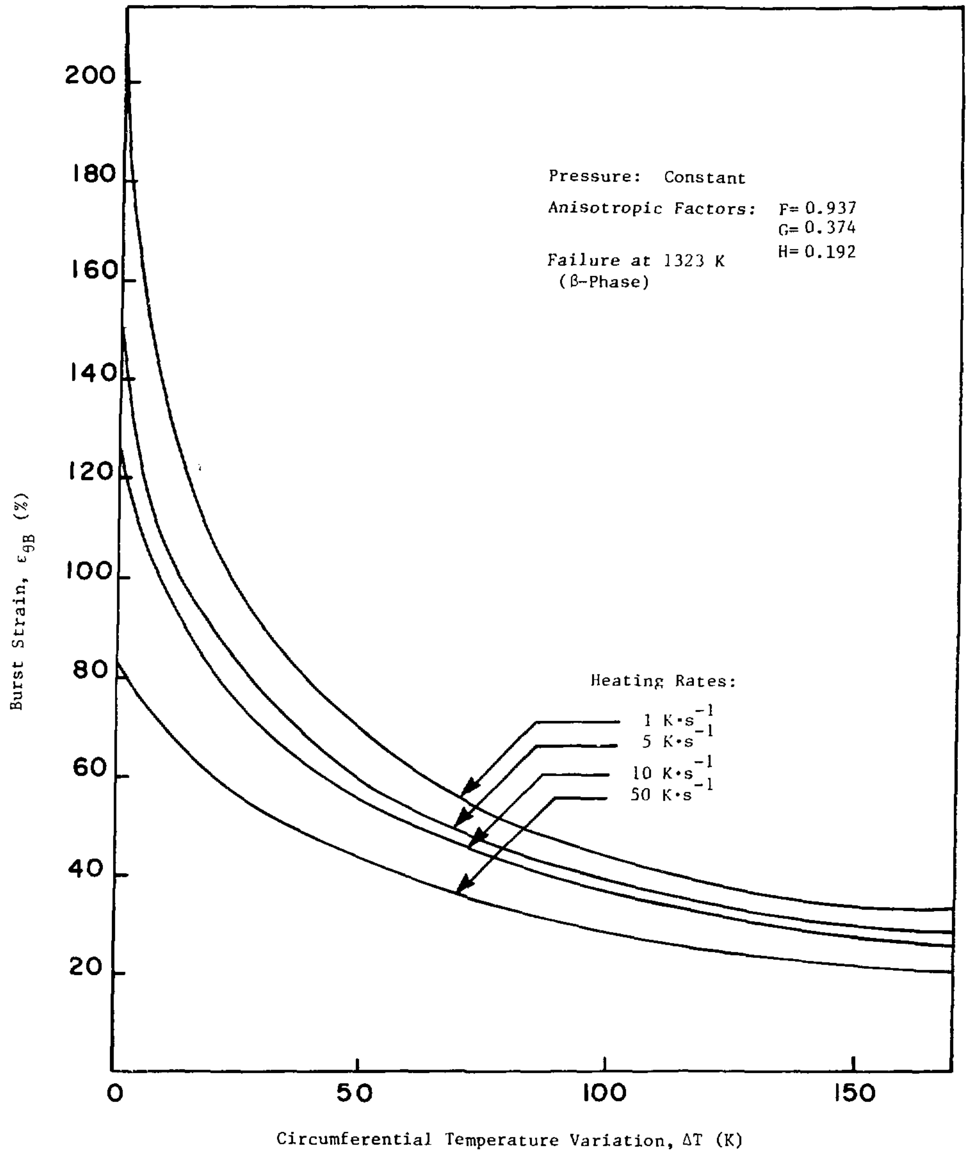


FIGURE 12: Effect of Heating Rate on the Burst Strain Versus Circumferential Temperature Variation for Failure in the β-Phase Region (1323 K)

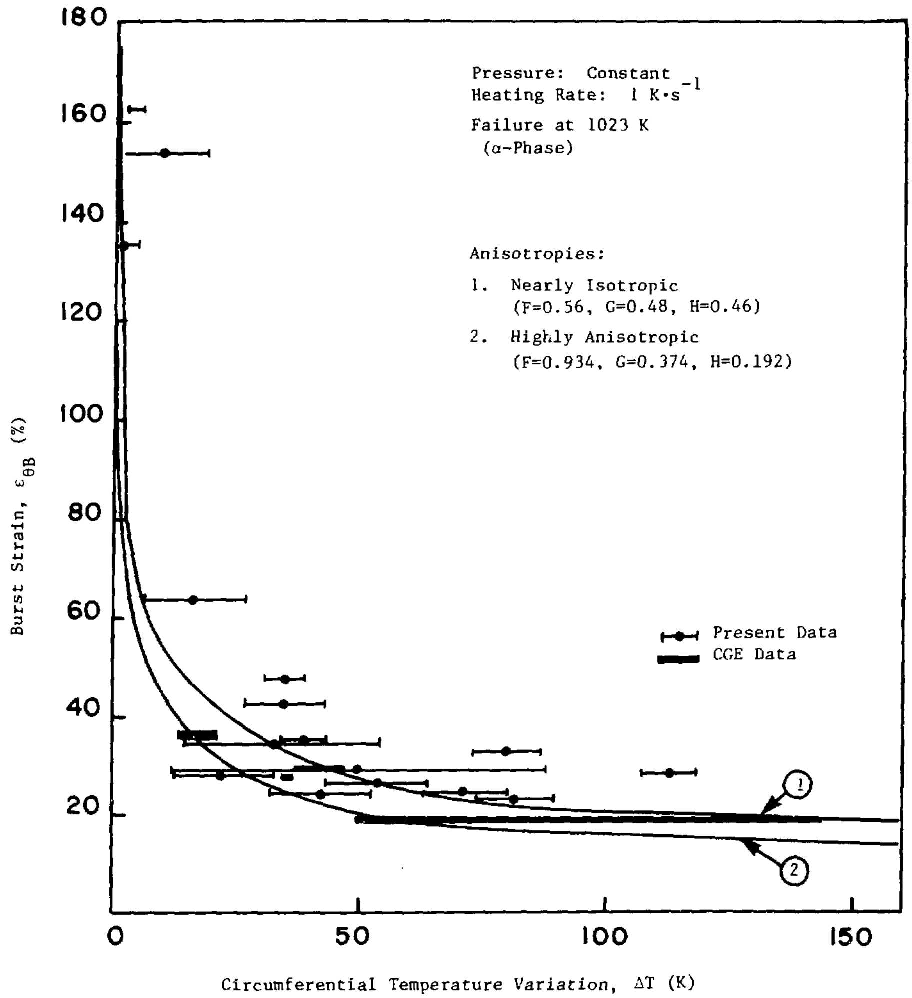


FIGURE 13: Effect of Anisotropy on the Burst Strain Versus Circumferential Temperature Variation for Failure in the α-Phase Region (1023 K)

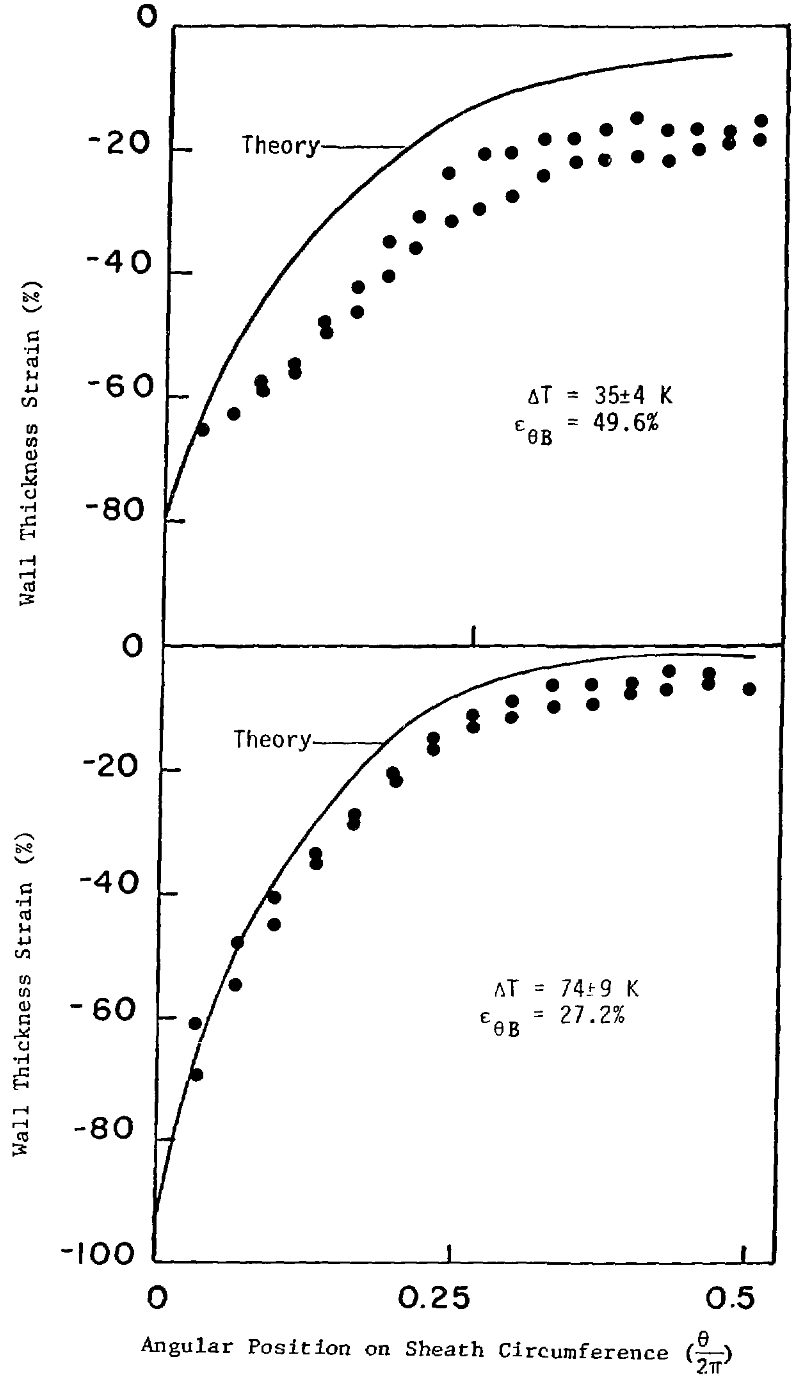


FIGURE 14: Wall Thickness Strain as a Function of the Angle Around the Sheath Circumference for Two Tests With Different Circumferential Temperature Variations

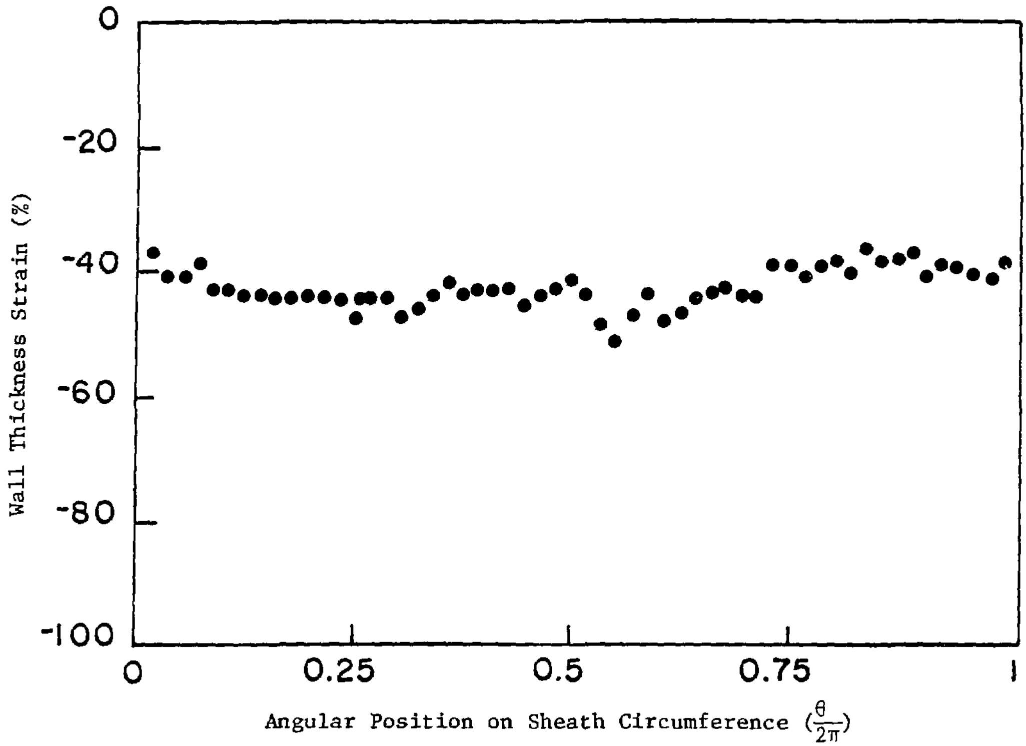


FIGURE 15: Wall Thickness Strain as a Function of the Angle Around the Sheath Circumference for a Test With Negligible (0±5 K) Circumferential Temperature Variation

ISSN 0067-0367

To identify individual documents in the series
we have assigned an AECL- number to each.

Please refer to the AECL- number when
requesting additional copies of this document
from

Scientific Document Distribution Office
Atomic Energy of Canada Limited
Chalk River, Ontario, Canada
KOJ 1JO

Price: $3.00 per copy

ISSN 0067-0367

Pour identifier les rapports individuels faisant partie de cette
série nous avons assigné un numéro AECL- à chacun.

Veuillez faire mention du numéro AECL -si vous
demandez d'autres exemplaires de ce rapport
au

Service de Distribution des Documents Officiels
L'Energie Atomique du Canada Limitée
Chalk River, Ontario, Canada
KOJ 1JO

prix: $3.00 par exemplaire